

Synthesis, Crystal Structures, and Magnetism of Cobalt Coordination Polymers Based on Dicyanamide and Pyrazine-dioxide Derivatives

Hao-Ling Sun, Zhe-Ming Wang, and Song Gao*

College of Chemistry and Molecular Engineering, State Key Laboratory of Rare Earth Materials Chemistry and Applications, PKU-HKU Joint Laboratory on Rare Earth Materials and Bioinorganic Chemistry, Peking University, Beijing 100871, China

Received November 23, 2004

Three coordination polymers of Co(II) with dicyanamide (dca) were obtained by adding coligands of 2,5-dimethylpyrazine-dioxide (2,5-dmpdo), 2,3,5-trimethylpyrazine-dioxide (2,3,5-tmpdo), or 2,3,5,6-tetramethylpyrazine-dioxide (2,3,5,6-tmpdo) to the binary system of Co-dca. $\text{Co}_2(\text{dca})_4(2,5\text{-dmpdo})_2$ (**1**) crystallizes in the triclinic space group $P\bar{1}$ with $a = 7.4962(2)$, $b = 9.0364(2)$, $c = 10.4783(4)$ Å, $\alpha = 72.567(1)$, $\beta = 72.557(1)$, $\gamma = 68.814(2)^\circ$, $V = 616.61(3)$ Å³, $Z = 1$, and $R1 = 0.0345$. $[\text{Co}_3(\text{dca})_6(\text{H}_2\text{O})_4] \cdot 2(2,3,5\text{-tmpdo})$ (**2**) is in the monoclinic space group $C2/c$ with $a = 29.477(1)$, $b = 7.3735(2)$, $c = 17.4631(7)$ Å, $\beta = 93.652(1)^\circ$, $V = 3787.9(2)$ Å³, $Z = 4$, and $R1 = 0.0532$. $[\text{Co}(\text{dca})_2(\text{H}_2\text{O})_2] \cdot 2(2,3,5,6\text{-tmpdo})$ (**3**) is in the monoclinic space group $P2_1/c$ with $a = 9.4739(3)$, $b = 11.3876(3)$, $c = 12.1778(3)$ Å, $\beta = 98.967(1)^\circ$, $V = 1297.74(6)$ Å³, $Z = 4$, and $R1 = 0.0481$. **1** contains an unusual (4, 4) Co-dca layer, representing a rare example of metal-dca coordination polymers with mixing 1,3- μ_2 - and 1,5- μ_2 -dca bridges. The Co-dca (4, 4) layers are connected by 2,5-dmpdo to give an α -Po-type network, which displays antiferromagnetic ordering below 10.8 K. **2** is a unique 3D framework composed of 2D twinned 1,5- μ_2 -dca bridged layers, which are connected by Co–H₂O–Co linkages. The noncoordinated 2,3,5-tmpdo units and the coordination water molecules form hydrogen-bonded chains that thread the framework. **3** has alternating stacks of usual Co-dca (4, 4) layers through 1,5- μ_2 -dca bridges and organic layers of noncoordinated 2,3,5,6-tmpdo. Weak antiferromagnetic and weak ferromagnetic coupling was observed in **2** and **3**, respectively.

Introduction

Coordination polymers based on dicyanamide (dca) bridging ligands have attracted much attention in the past few years not only because of their interesting extended architectures but also because they can help us understand the fundamentals of magnetic coupling and magneto-structure correlation.^{1–12} The dca ligand has shown extreme coordination versatility. It can act as a terminal ligand through a nitrile nitrogen,¹ a potential 1,3- μ_2 bridge through the amido nitrogen and one nitrile nitrogen, an end-to-end 1,5- μ_2 bridge through two nitrile nitrogen atoms,² a three-atom μ_3 bridge through all of the nitrogen atoms,³ an unusual μ_4 -1,1,3,5 bridge with one of the two nitrile nitrogen atoms connected to two metal ions⁴, and a μ_5 -1,1,3,5,5 bridge with both nitrile

atoms connected to two metal centers.⁵ The coordination versatility, together with the coordination nature of the central

* Corresponding author. Tel: 0086–10–62756320. Fax: 0086–10–62751708. E-mail: gaosong@pku.edu.cn.

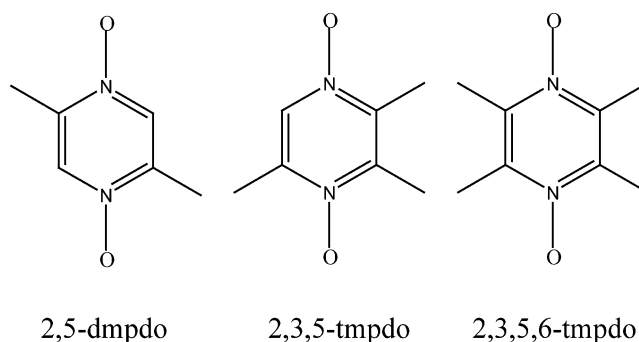
(1) (a) Potocnak, I.; Dunaj-Jurco, M.; Miklos, D.; Kabesova, M.; Jager, L. *Acta Crystallogr., Sect. C* **1995**, *51*, 600. (b) Dasna, I.; Golhen, L.; Pena, O.; Daro, N.; Sutter, J. P. *C. R. Acad. Sci. Ser. IIc: Chim.* **2001**, *4*, 125.

- (2) (a) Sun, B. W.; Gao, S.; Ma, B. Q.; Niu, D. Z.; Wang, Z. M. *J. Chem. Soc., Dalton Trans.* **2000**, 4187. (b) Wang, Z. M.; Sun, B. W.; Luo, J.; Gao, S.; Liao, C. S.; Yan, C. H.; Li, Y. *Polyhedron* **2003**, *22*, 433. (c) Sun, B. W.; Gao, S.; Ma, B. Q.; Wang, Z. M. *Inorg. Chem. Commun.* **2001**, *4*, 72. (d) Wang, Z. M.; Sun, B. W.; Luo, J.; Gao, S.; Liao, C. S.; Yan, C. H.; Li, Y. *Inorg. Chim. Acta* **2002**, *332*, 127. (e) Yeung, W. F.; Gao, S.; Wong, W. T.; Lau, T. C. *New J. Chem.* **2002**, 523. (f) Manson, J. L.; Huang, Q. Z.; Lynn, J. W.; Koo, H. J.; Whangbo, M. H.; Bateman, R.; Otsuka, T.; Wada, N.; Argyriou, D. N.; Miller, J. S. *J. Am. Chem. Soc.* **2001**, *123*, 162. (g) van der Werff, P. M.; Batten, S. R.; Jensen, P.; Moubaraki, B.; Murray, K. S. *Inorg. Chem.* **2001**, *40*, 1718.
- (3) (a) Batten, S. R.; Jensen, P.; Moubaraki, B.; Murray, K. S.; Rubson, R. *Chem. Commun.* **1998**, 439. (b) Manson, J. L.; Kmetz, C. R.; Huang, Q. Z.; Lynn, J. W.; Bendele, G. M.; Pagola, S.; Stephens, P. W.; Liable-Sands, L. M.; Rheingold, A. L.; Epstein, A. J.; Miller, J. S. *Chem. Mater.* **1998**, *10*, 2552. (c) Kurmoo, M.; Kepert, C. J. *New J. Chem.* **1998**, 1515. (d) Kmetz, C. R.; Huang, Q. Z.; Lynn, J. W.; Erwin, R. W.; Manson, J. L.; McCall, S.; Crow, J. E.; Stevenson, K. L.; Miller, J. S.; Epstein, A. J. *Phys. Rev B* **2000**, *62*, 5576. (e) Manson, J. L.; Kmetz, C. R.; Palacio, F.; Epstein, A. J.; Miller, J. S. *Chem. Mater.* **2001**, *13*, 1068. (f) Miller, J. S.; Manson, J. L. *Acc. Chem. Res.* **2001**, *34*, 563.
- (4) Chow, Y. M.; Britton, D. *Acta Crystallogr., Sect. B* **1975**, *31*, 1934.

metal ions, has allowed the possibility of the construction of different architectures displaying diverse magnetic properties.

The binary systems of dca exhibit either a 3D rutile-like structure³ or a 2D layer with a tetrahedral coordination environment.⁶ They show different magnetic properties such as ferromagnetism, weak ferromagnetism, and paramagnetism,³ depending on the metal in the system.⁶ The introduction of coligands, especially ditopic ones, such as pyrazine, 4,4'-bipyridine, and their derivatives to the binary system, have led to dramatic modification of the crystal structure and magnetic properties. A lot of compounds containing transition metals, dca, and coligands were reported. If one takes only the framework constructed by dca into account, then the polymeric topologies of metal-dca include a 1D linear chain with a double 1,5- μ_2 -dca bridge,⁷ the 1D nanotube-like structure with both a 1,5- μ_2 - and a μ_3 -dca bridge,⁸ a 2D (4, 4) net with a single 1,5- μ_2 -dca bridge,⁹ a 2D triangular lattice with both a 1,5- μ_2 - and a μ_3 -dca bridge¹⁰, and a herringbone-like lattice with a 1,5- μ_2 -dca bridge,¹¹ and various magnetic behaviors were observed. We have reported some works about the crystal engineering and magnetism of coordination polymers previously in which the pyrazine-dioxide (pzdo) or one of its derivatives, 2-methylpyrazine-dioxide (2-mpdo), was introduced into the binary Co-dca system.^{10b,12} The coordination polymers show a rare triangle Co-dca layer constructed of both 1,5- μ_2 - and μ_3 -dca with long-range ferromagnetic ordering below 2.5 K. In this work, to elucidate the size, shape, and coordination ability of the pyrazine-dioxide derivatives in tuning the crystal structure and mediating magnetic interplay, we chose three other methyl-substituted derivatives of pzdo, namely, 2,5-dimethylpyrazine-dioxide (2,5-dmpdo), 2,3,5-trimethylpyrazine-dioxide (2,3,5-tmpdo), and 2,3,5,6-tetramethylpyrazine-dioxide (2,3,5,6-tmpdo) (Scheme 1), to obtain successfully three Co(II) complexes, $\text{Co}_2(\text{dca})_4(2,5\text{-dmpdo})_2$ **1**, $[\text{Co}_3(\text{dca})_6(\text{H}_2\text{O})_4] \cdot 2(2,3,5\text{-tmpdo})$ **2**, and $[\text{Co}(\text{dca})_2(\text{H}_2\text{O})_2] \cdot 2(2,3,5,6\text{-$

Scheme 1



tmpdo) **3**, and characterize them structurally and magnetically. The three compounds are based on the Co-dca (4, 4) network. They are of much interest because of their unique structures, the role of pzdo derivatives in interfering with the structures, and their interesting magnetic properties.

Experimental Section

Elemental analyses of carbon, hydrogen, and nitrogen were carried out with an Elementar Vario EL. FTIR spectra were obtained using pure samples of the three compounds in the range of 4000 to 650 cm^{-1} on a Nicolet Magna 750 FT/IR spectrometer. Reflectance UV-vis spectra were recorded on a SHIMADZU UV-3100 spectrophotometer with an integrated sphere attachment at 200–800 nm against ground powder samples of the compounds and upon a BaSO_4 background. Variable-temperature magnetic susceptibility, zero-field ac magnetic susceptibility measurements, and field dependence magnetization of **1** and **2** were performed on an Oxford MagLab2000 system.¹³ Magnetic property measurements for **3** were carried out on a Quantum Design MPMS-XL5 SQUID system. The experimental susceptibilities were corrected for the diamagnetism of the constituent atoms (Pascal's tables)¹⁴ and the background of the sample holder.

Synthesis. 2,5-dmpdo, 2,3,5-tmpdo, and 2,3,5,6-tmpdo were prepared from 2,5-dimethylpyrazine, 2,3,5-trimethylpyrazine, and 2,3,5,6-tetramethylpyrazine by the literature method.¹⁵ Sodium dicyanamide ($\text{Na}(\text{dca})$) and other chemicals were purchased and used without further purification.

$\text{Co}_2(\text{dca})_4(2,5\text{-dmpdo})_2$ (1**).** $\text{CoCl}_2 \cdot 6\text{H}_2\text{O}$ (0.25 mmol, 60 mg) and 0.50 mmol (45 mg) of $\text{Na}(\text{dca})$ were dissolved in 5 mL of water. An aqueous solution of 2,5-dmpdo (0.25 mmol, 35 mg, 5 mL) was added while stirring. The resulting solution was filtrated and allowed to evaporate slowly at room temperature. Deep-red block crystals appeared overnight. The crystals were washed with water and air dried (yield 85%). Anal. Calcd for $\text{C}_{20}\text{H}_{16}\text{Co}_2\text{N}_{16}\text{O}_4$: C, 36.27; H, 2.43; N, 33.84%. Found: C, 35.96; H, 2.38; N, 33.68%. IR (cm^{-1}): 2303 (ms), 2281 (ms), 2257 (ms), 2240 (m), 2183 (s). UV-vis (cm^{-1}): 20 500 br (Figure S1).¹⁶

$[\text{Co}_3(\text{dca})_6(\text{H}_2\text{O})_4] \cdot 2(2,3,5\text{-tmpdo})$ (2**).** A procedure similar to that used for compound **1**, with 2,3,5-tmpdo instead of 2,5-dmpdo,

- (5) Shi, Y. J.; Chen, X. T.; Li, Y. Z.; Xue, Z. L.; You, X. Z. *New J. Chem.* **2002**, 26, 1711.
- (6) Manson, J. L.; Lee, D. W.; Rheingold, A. L.; Miller, J. S. *Inorg. Chem.* **1998**, 37, 5966.
- (7) (a) Gao, E. Q.; Wang, Z. M.; Liao, C. S.; Yan, C. H. *New J. Chem.* **2002**, 26, 1096. (b) Dasna, I.; Golhen, S.; Ouahab, L.; Pena, O.; Guillevic, J.; Fettouhi, M. *J. Chem. Soc., Dalton Trans.* **2000**, 129. (c) Batten, S. R.; Jensen, P.; Kepert, C. J.; Kurmoo, M.; Moubaraki, B.; Murray, K. S.; Price, D. J. *J. Chem. Soc., Dalton Trans.* **1999**, 2987. (d) Escuer, A.; Mautner, F. A.; Sanz, N.; Vicente, R. *Inorg. Chem.* **2000**, 39, 1668.
- (8) Jensen, P.; Batten, S. R.; Moubaraki, B.; Murray, K. S. *Chem. Commun.* **2000**, 793.
- (9) (a) Dasna, I.; Golhen, S.; Ouahab, L.; Fettouhi, M.; Pena, O.; Daro, N.; Sutter, J. P. *Inorg. Chim. Acta* **2001**, 326, 37. (b) Manson, J. L.; Schlueter, J. A.; Geiser, U.; Stone, M. B.; Reich, D. H. *Polyhedron* **2001**, 20, 1423. (c) Dasna, I.; Golhen, S.; Ouahab, L.; Pena, O.; Daro, N. *Chemistry* **2001**, 4, 125.
- (10) (a) Kutasi, A. M.; Batten, S. R.; Moubaraki, B.; Murray, K. S. *J. Chem. Soc., Dalton Trans.* **2002**, 819. (b) Sun, H. L.; Gao, S.; Ma, B. Q.; Su, G. *Inorg. Chem.* **2003**, 42, 5399.
- (11) Luo, J. H.; Hong, M. C.; Weng, J. B.; Zhao, Y. J.; Cao, R. *Inorg. Chim. Acta* **2002**, 329, 59.
- (12) (a) Ma, B. Q.; Sun, H. L.; Gao, S.; Su, G. *Chem. Mater.* **2001**, 13, 1946. (b) Sun, H. L.; Ma, B. Q.; Gao, S.; Su, G. *Chem. Commun.* **2001**, 2586. (c) Sun, H. L.; Gao, S.; Ma, B. Q.; Chang, F.; Fu, W. F. *Microporous Mesoporous Mater.* **2004**, 73, 89. (d) Sun, H. L.; Gao, S.; Ma, B. Q.; Su, G.; Batten, S. R. *Cryst. Growth Des.* **2005**, 5, 269.

- (13) *MagLab 2000* system, a multifunctional physical property measurement system including dc/ac magnetic measurements, resistance and heat capacity measurements, and so forth in the 1.8–400 K temperature range and ± 7 T superconductor magnetic field; Oxford Instruments.
- (14) *Theory and Application of Molecular Paramagnetism*; Boudreaux, E. A., Mulay, J. N., Eds.; J. Wiley and Sons: New York, 1976.
- (15) Simpon, P. G.; Vinciguerra, A.; Quagliano, J. V. *Inorg. Chem.* **1963**, 2, 282.
- (16) (a) Manson, J. L.; Kmety, C. R.; Huang, Q. W.; Lynn, Z. J.; Bendele, G. M.; Pagola, S.; Stephens, P. W.; Liable-Sands, L. M.; Rheingold, A. L.; Epstein, A. J.; Miller, J. S. *Chem. Mater.* **1998**, 10, 2552. (b) Kurmoo, M.; Kepert, C. J. *New J. Chem.* **1998**, 1515.

Table 1. Crystal Data and Structure Refinement for **1–3**

	1	2	3
formula	C ₂₀ H ₁₆ Co ₂ N ₁₆ O ₄	C ₂₆ H ₂₈ Co ₃ N ₂₂ O ₈	C ₂₀ H ₂₈ CoN ₁₀ O ₆
fw	662.35	953.49	563.45
cryst syst	triclinic	monoclinic	monoclinic
space group	P1	C2/c	P2 ₁ /c
a (Å)	7.4962(2)	29.477(1)	9.4739(3)
b (Å)	9.0364(2)	7.3735(2)	11.3876(3)
c (Å)	10.4783(4)	17.4631(7)	12.1778(3)
α (deg)	72.567(1)	90	90
β (deg)	72.557(1)	93.652(1)	98.967(1)
γ (deg)	68.814(2)	90	90
V (Å ³)	616.61(3)	3787.9(2)	1297.74(6)
Z	1	4	2
D _{calcd} (Mg/m ³)	1.784	1.672	1.442
μ (mm ⁻¹)	1.412	1.377	0.716
GOF	1.030	1.020	1.023
F(000)	334	1932	586
data collected	13996	26327	22645
unique data	2769	4329	2901
observed data (I > 2σ(I))	1896	2729	2034
R _{int}	0.0633	0.0878	0.0721
R1 (I > 2σ(I)) ^a	0.0345	0.0532	0.0481
wR2 (I > 2σ(I)) ^b	0.0675	0.1061	0.1266
R1 (all data) ^a	0.0730	0.1085	0.0785
wR2 (all data) ^b	0.0820	0.1221	0.1410

$$^a R1 = \sum ||F_o| - |F_c|| / \sum |F_o|, \quad ^b wR2 = [\sum w(F_o^2 - F_c^2)^2] / \sum w(F_o^2)^{1/2}.$$

was used to prepare compound **2**. Purple block crystals were obtained after crystallization for 1 month (yield 70%). Anal. Calcd for C₂₆H₂₈Co₃N₂₂O₈: C, 32.75; H, 2.96; N, 32.32%. Found: C, 32.76; H, 3.17; N, 32.15%. IR (cm⁻¹): 2311 (m), 2262 (m), 2187 (s). UV–vis (cm⁻¹): 18 800, 19 800 (Figure S1).¹⁶

[Co(dca)₂(H₂O)₂]₂·2(2,3,5,6-tmpdo) (**3**). A procedure similar to that used for compound **1**, with 2,3,5,6-tmpdo instead of 2,5-dmpdo, was used to prepare compound **3**. Red block crystals were obtained after 2 weeks (yield 75%). Anal. Calcd for C₂₀H₂₈CoN₁₀O₆: C, 42.63; H, 5.01; N, 24.86%. Found: C, 42.70; H, 5.02; N, 24.52%. IR (cm⁻¹): 2307 (m), 2259 (m), 2195 (s). UV–vis (cm⁻¹): 20 100 br (Figure S1).¹⁶

Crystallography. Intensity data for crystals of **1–3** were collected on a Nonius Kappa CCD diffractometer with graphite-monochromated Mo Kα radiation (0.71073 Å) at 293 K. The structures were solved by direct methods and refined by a full-matrix least-squares technique based on *F*² using the SHELXL 97 program.¹⁷ All of the non-hydrogen atoms were refined anisotropically. The hydrogen atoms of water molecules were located using a difference Fourier map and refined with constraints for the ideal geometry of a water molecule with the O–H distance of 0.96 Å, the H–O–H angle of 105°, and one overall isotropic thermal parameter. Other hydrogen atoms were placed by calculation positions. The details of the crystal data and the selected bond lengths and angles for compounds **1–3** are listed in Tables 1 and 2, respectively.

Results and Discussion

Description of the Structures. Structure of Co₂(dca)₄·(2,5-dmpdo)₂ (1**).** As shown in Figure 1, the structure of compound **1** has two crystallographically independent Co(II) ions, both lying at inversion centers but possessing different coordination octahedra. The Co1 atom is coordinated by two nitrile nitrogen atoms [Co–N = 2.065 Å], two amide

(17) Sheldrick, G. M. *SHELXS-97*, PC version; University of Göttingen: Göttingen, Germany, 1997.

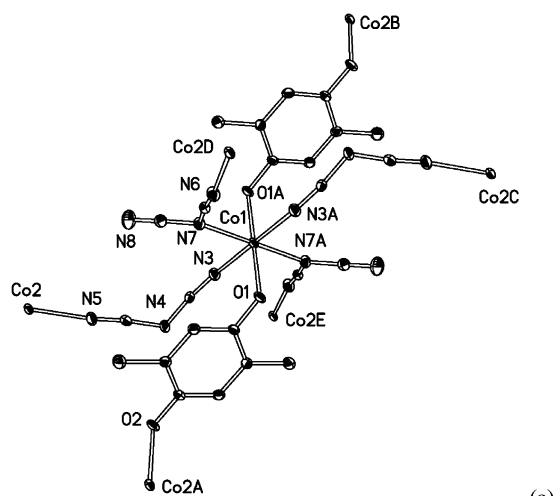
Table 2. Selected Bond Lengths (Å) and Angles (deg) for **1–3**

		1^a	
Co(1)–N(3)	2.065(2)	Co(1)–O(1)	2.122(2)
Co(1)–N(7)	2.178(2)	Co(2)–N(6)b	2.089(2)
Co(2)–N(5)	2.105(2)	Co(2)–O(2)e	2.112(2)
N(3)a–Co(1)–N(3)	180.0	N(3)–Co(1)–O(1)	90.62(7)
N(3)–Co(1)–O(1)a	89.38(7)	O(1)–Co(1)–O(1)a	180.0
N(3)a–Co(1)–N(7)	91.27(8)	N(3)–Co(1)–N(7)	88.73(8)
O(1)–Co(1)–N(7)	88.35(7)	O(1)–Co(1)–N(7)a	91.65(7)
N(7)–Co(1)–N(7)a	180.0	N(6)b–Co(2)–N(6)c	180.00
N(6)b–Co(2)–N(5)	87.32(8)	N(6)c–Co(2)–N(5)	92.68(8)
N(5)–Co(2)–N(5)d	180.00	N(6)b–Co(2)–O(2)e	87.53(7)
N(6)c–Co(2)–O(2)e	92.47(7)	N(5)–Co(2)–O(2)e	88.03(7)
N(5)–Co(2)–O(2)f	91.97(7)	O(2)e–Co(2)–O(2)f	180.0
		2^b	
Co(1)–N(4)	2.042(4)	Co(1)–N(1)	2.057(3)
Co(1)–N(6)a	2.062(3)	Co(1)–N(7)	2.081(3)
Co(1)–O(2)	2.235(2)	Co(1)–O(1)	2.312(2)
Co(2)–N(9)	2.088(4)	Co(2)–N(3)c	2.111(3)
Co(2)–O(3)	2.127(3)	N(4)–Co(1)–N(1)	94.70(13)
N(4)–Co(1)–N(6)a	98.19(13)	N(1)–Co(1)–N(6)a	95.83(13)
N(4)–Co(1)–N(7)	91.88(13)	N(1)–Co(1)–N(7)	171.00(13)
N(6)a–Co(1)–N(7)	89.27(13)	N(4)–Co(1)–O(2)	168.31(12)
N(1)–Co(1)–O(2)	88.44(9)	N(6)a–Co(1)–O(2)	92.67(11)
N(7)–Co(1)–O(2)	83.92(9)	N(4)–Co(1)–O(1)	89.54(12)
N(1)–Co(1)–O(1)	82.86(9)	N(6)a–Co(1)–O(1)	172.25(11)
N(7)–Co(1)–O(1)	91.09(9)	O(2)–Co(1)–O(1)	79.67(9)
N(9)–Co(2)–N(9)b	180.0	N(9)–Co(2)–N(3)c	89.50(13)
N(9)–Co(2)–N(3)d	90.50(13)	N(3)c–Co(2)–N(3)d	180.0
N(9)–Co(2)–O(3)	91.40(12)	N(9)–Co(2)–O(3)b	88.60(12)
O(3)–Co(2)–O(3)b	180.0		
		3^c	
Co1–O3	2.097(2)	Co1–N3	2.097(3)
Co1–N5b	2.100(2)		
O3a–Co1–O3	180.0	O3a–Co1–N3	89.46(10)
O3–Co1–N3	90.54(10)	N3–Co1–N3a	180.0
N3–Co1–N5c	91.39(11)	O3–Co1–N5c	90.72(9)
O3–Co1–N5b	89.28(9)	N3–Co1–N5b	88.61(11)
N5b–Co1–N5c	180.0		

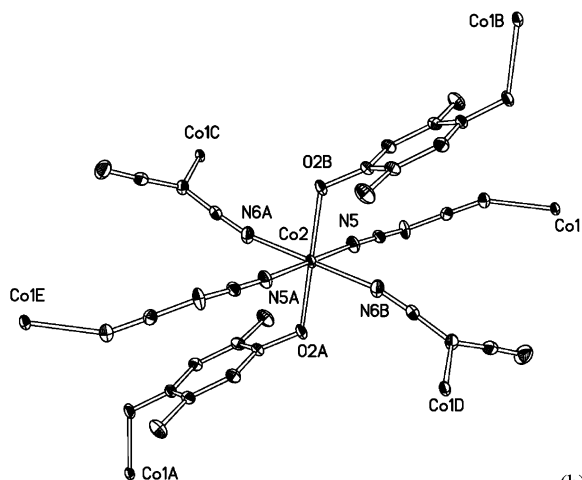
^a Symmetry code: a $-x, -y, -z$; b $-x, -y - 1, -z$; c $x, y, z - 1$; d $-x, -y - 1, -z - 1$; e $-x + 1, -y - 1, -z - 1$; f $x - 1, y, z$. ^b Symmetry code: a $x, y - 1, z$; b $-x + 1/2, -y + 1/2, -z$; c $x - 1/2, y - 1/2, z$; d $-x + 1, -y + 1, -z$. ^c Symmetry code: a $-x + 1, -y, -z + 1$; b $-x + 1, y - 1/2, -z + 3/2$; c $x, -y + 1/2, z - 1/2$.

nitrogen atoms [Co–N = 2.178 Å] from four dca at equatorial positions, and two oxygen atoms of two 2,5-dmpdo [Co–O = 2.122 Å] at axial sites. The Co2 is coordinated, however, by four nitrile nitrogen atoms at equatorial sites [Co–N = 2.089 or 2.105 Å] and two oxygen atoms of 2,5-dmpdo at axial sites [Co–O = 2.112 Å]. Each Co1 is connected to two Co2 atoms through 1,3- μ_2 -dca and another two Co2 atoms through 1,5- μ_2 -dca and vice versa, forming a 2D (4, 4) sheet parallel the *bc* plane (Figure 2). These sheets are then linked into an α -Po-type network via axially bound 2,5-dmpdo “pillars” (Figure S2), which is similar to the related network, such as M(dca)₂L, L = pyrazine (α form), 4,4'-bipyridine, containing 2D (4, 4) sheets of M(dca)₂ bridged by bidentate pillars.¹⁸ The large angular deviation of the bridge of 2,5-dmpdo from perpendicular to the sheets

(18) (a) Jensen, P.; Batten, S. R.; Moubaraki, B. K.; Murray, S. J. *Solid State Chem.* **2001**, 159, 352. (b) Jensen, P.; Batten, S. R.; Moubaraki, B. K.; Murray, S. J. *Chem. Soc., Dalton Trans.* **2002**, 3712. (c) Manson, J. L.; Incarvito, C. D.; Rheingold, A. L.; Miller, J. S. *J. Chem. Soc., Dalton Trans.* **1998**, 3705. (d) Sun, B. W.; Gao, S.; Ma, B. Q.; Wang, Z. M. *New J. Chem.* **2000**, 24, 953. (e) Martin, S.; Barandika, M. G.; Ezpeleta, J. M.; Cortes, R.; de Larramendi, J. I. R.; Lezama, L.; Rojo, T. *J. Chem. Soc., Dalton Trans.* **2002**, 4275.



(a)



(b)

Figure 1. Coordination environment of Co1 (a) and Co2 (b) in **1**.

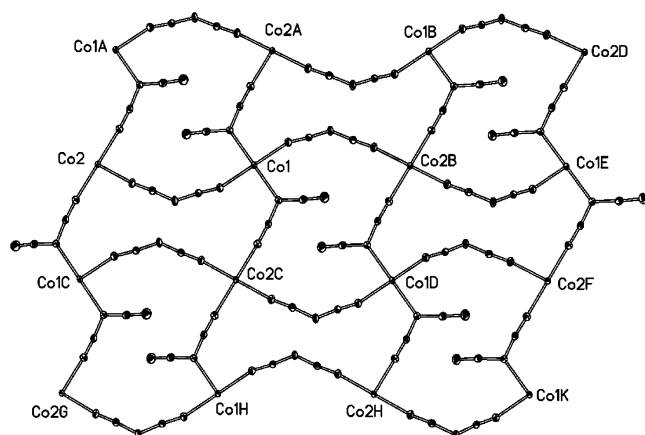
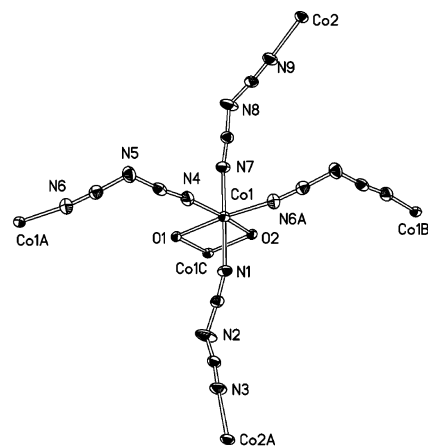
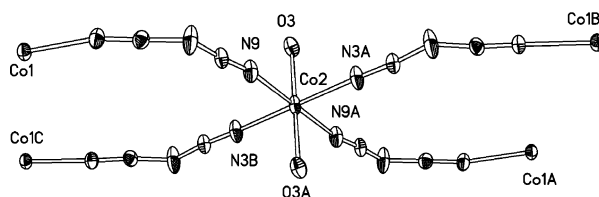


Figure 2. Two-dimensional (4, 4) layer in **1** formed by 1,3- μ - and 1,5- μ -dca bridges.

is due mainly to the bend around the coordinating oxygen ($\text{N1-O1-Co1} = 120.5^\circ$). This also has an effect of bringing the (4, 4) sheets closer together, making the net less spacious, and thus only one net is formed without interpenetration. The $\text{Co}\cdots\text{Co}$ separations through 1,3- μ_2 -dca, 1,5- μ_2 -dca, and μ -2,5-dmpdo are 5.803, 7.877, and 8.379 Å, respectively. The $\text{Co}\cdots\text{Co}$ separations through 1,3- μ_2 -dca are a little shorter than those through μ_3 -dca found in the compounds



(a)

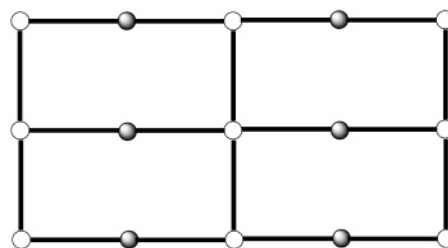


(b)

Figure 3. Coordination environment of Co1 (a) and Co2 (b) in **2**.



(a)



○ Co1 ● Co2 — dca

(b)

Figure 4. (a) Unique double layer based on 1,5- μ -dca found in **2**. (b) Schematic view of the (4, 4) net. In the double layer, the two (4, 4) nets are twinned via Co2.

of 3D $\text{M}(\text{dca})_2$, $\text{M}(\text{dca})_2(\text{H}_2\text{O})(\text{L})$ ($\text{M} = \text{Ni}, \text{Co}$; $\text{L} =$ phenazine), and $\text{Co}(\text{dca})_2(\text{L})$ ($\text{L} =$ pyrazine-dioxide and 2-methylpyrazine-dioxide).^{4,10} The $\text{Co}\cdots\text{Co}$ separations through 1,5- μ_2 -dca and μ -2,5-dmpdo are similar to those found in the reported compounds.^{2,6-12}

Structure of $[\text{Co}_3(\text{dca})_6(\text{H}_2\text{O})_4] \cdot 2(2,3,5\text{-tmpdo})$ (2**).** The unique feature of this structure is the interesting twinned Co-dca double layers, which are further linked by coordination water molecules via $\text{Co-H}_2\text{O-Co}$ linkages (Figures 3–6), and the 2,3,5-tmpdo units occupy the open windows of the layers. In the structure, the two unique $\text{Co}(\text{II})$ ions, Co1 and Co2 (Figure 3), are all octahedrally coordinated by four nitrile nitrogen atoms from four dca ligands and two water molecules. However, Co1 in the general position (Wyckoff

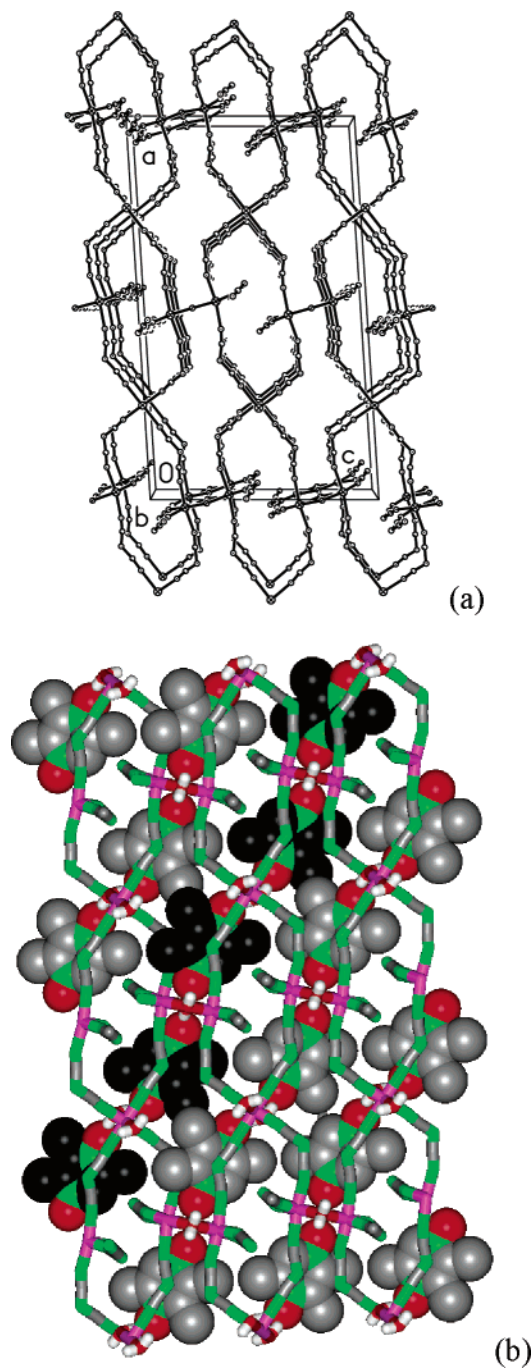


Figure 5. (a) Three-dimensional network constructed by double μ -H₂O between the unique 2D framework based on 1,5- μ -dca in **2**. (b) Three-dimensional structure of **2** with emphasized threading of the H-bonded 2,3,5-tmpdo-water chains in the framework.

8f) has its two water molecules in *cis* positions, whereas Co₂, located at the crystallographic inversion center (Wyckoff 4c), has two water molecules in *trans* positions. Therefore, Co1N₄ is a saddle-like moiety, whereas Co₂N₄ is a planar-square one. The bond distances around Co1 are Co–N = 2.042–2.081 Å and Co–O = 2.312–2.235 Å, whereas those around Co2 are Co–N = 2.088–2.111 Å and Co–O = 2.127 Å. Both Co ions are connected through 1,5- μ -dca ligands to form a unique 2D structure (Figure 4a) in which each Co2 links four Co1 ions and each Co1 links two Co1 and two Co2 ions, respectively. The structure is best described as

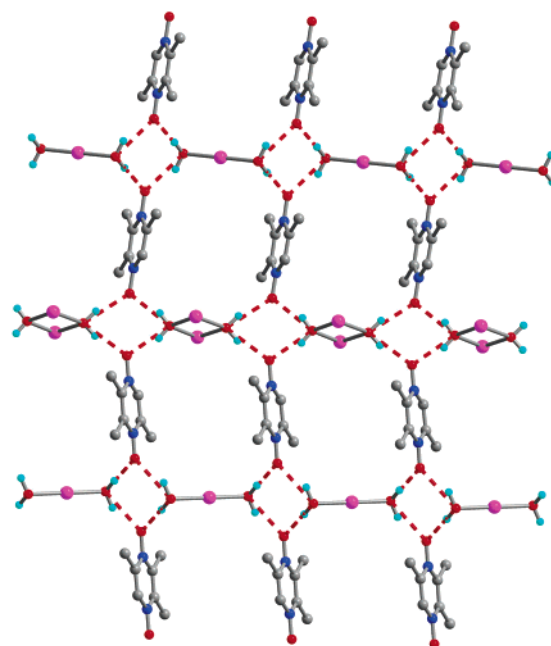


Figure 6. Two-dimensional layer formed by the double hydrogen bonding between solvent 2,3,5-tmpdo and the coordination water molecule in **2**.

Table 3. Hydrogen Bonding Parameters in **2** and **3**

D–H···A	D–H (Å)	H···A (Å)	D···A (Å)	D–H···A (deg)
2^a				
O1–H1w···O4a	0.897	1.997	2.868	163.70
O2–H2w···O4a	0.849	1.914	2.731	160.84
O3–H3w···O5b	0.921	1.960	2.797	150.34
O3–H4w···O5c	0.962	1.851	2.805	171.03
3^b				
O3–H2w···O1a	0.950	1.746	2.682	167.80
O3–H1w···O2b	0.943	1.787	2.713	166.51

^a Symmetry codes: a $-x + 1, y + 1, -z + 1/2$; b $-x + 1/2, y - 1/2, -z + 1/2$; c $x, -y, z - 1/2$. ^b Symmetry codes: a $x - 1, -y + 1/2, z - 1/2$; b $-x + 1, -y + 1, -z + 1$.

twinned double layers of the two (4, 4) networks (Figure 4b) through sharing their Co₂ sites, which have the two *trans* coordination water molecules in the middle of the layer. The (4, 4) network has nodes of Co1 and rectangular windows with two short edges of Co1–dca–Co1, whereas the two long edges are Co1–dca–Co2–dca–Co1 linkages. Within the layer, the Co···Co distances, spanned by dca ligands, are 7.716 Å for Co1···Co1 and 8.510 Å for Co1···Co2. Therefore, the window is 17.02 Å long and 7.72 Å wide. The layers are parallel to the *ab* plane. They are further linked by the double μ -H₂O bridges between the two Co1 atoms along the *c* axis with a Co···Co separation of 3.490 Å, producing a unique 3D framework (Figure 5a). It is important to point out that in the framework the rectangular windows of the layers form channels along the *c* axis with the coordination H₂O (O3 to Co2) molecules inside the channel. The channels are occupied by noncoordinated 2,3,5-tmpdo (Figure 5b). The two N-oxides of 2,3,5-tmpdo are involved in the hydrogen bonding patterns of R₄²(8) with the coordinated water molecules (Figure 6).¹⁹ With these hydrogen bonds (Table

(19) (a) Etter, M. C. *Acc. Chem. Res.* **1990**, *23*, 120. (b) Bernstein, J.; Davis, R. E.; Shimoni, L.; Chang, N. L. *Angew. Chem., Int. Ed. Engl.* **1995**, *34*, 1555.

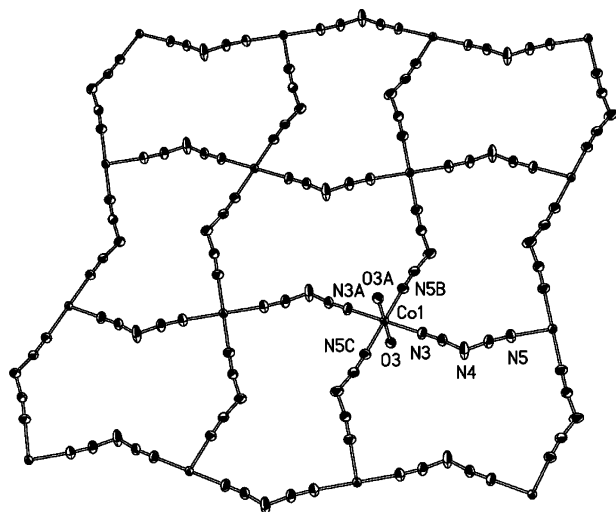


Figure 7. Two-dimensional (4, 4) sheet in **3**.

3), the noncoordinated 2,3,5-tmpdo units and the coordination water molecules form the hydrogen-bonded chains that thread the framework (Figure 5b).

Structure of $[\text{Co}(\text{dca})_2(\text{H}_2\text{O})_2] \cdot 2(2,3,5,6\text{-tmpdo})$ (3**).** The structure of **3** is a laminar type, consisting of alternating stacks of 2D (4, 4) sheets of $\text{Co}(\text{dca})_2$ (Figure 7) and organic layers of noncoordinated 2,3,5,6-tmpdo. Within the $\text{Co}(\text{dca})_2$ sheet, the octahedral $\text{Co}(\text{II})$ ion is coordinated by four nitrile nitrogens in equatorial positions ($\text{Co}-\text{N} = 2.097\text{--}2.100 \text{ \AA}$) and two water molecules in axial sites ($\text{Co}-\text{O} = 2.097 \text{ \AA}$). The metal ions are connected by single 1,5- μ_2 -dca bridges between the metal sites, as observed in several compounds containing this kind of $\text{M}(\text{dca})_2$ sheet. The sheet has square windows of $8.336 \times 8.336 \text{ \AA}^2$ based on the $\text{Co} \cdots \text{Co}$ distances. The organic layer, composed of noncoordinated 2,3,5,6-tmpdo units, has a packing pattern (Figure S3) in which the organic molecules are in face-to-face dimers by π - π stacking²⁰ with an interplane distance of ca. 3.58 \AA , and the adjacent dimers are rotated by ca. 90° with respect to each other, similar to the packing style of organic donors in κ -type organic superconductors.²¹ The 3D structure is composed of alternating stacks of $\text{Co}(\text{dca})_2$ sheets and organic 2,3,5,6-tmpdo layers. The two kinds of layers are linked by strong hydrogen bonding (Table 3) between the coordination water molecule and the *N*-oxides of 2,3,5,6-tmpdo (Figure S4).

This work, together with our previously reported results, gives us the chance to explore systematically the role of coligands of pzdo and its methyl derivatives in tuning the crystal structure of Co-dca systems. The crystal structures of **1–3** are quite different from our previously reported $\text{Co}(\text{dca})_2\text{L}$ with $\text{L} = \text{pzdo}$ and 2-mpdo,^{10b} both containing

(20) Janiak, C. J. *Chem. Soc., Dalton Trans.* **2000**, 3885.

(21) (a) Kobayashi, A.; Udagawa, T.; Tomita, H.; Naito, T.; Kobayashi, H. *Chem. Lett.* **1993**, 2179. (b) Kini, A. M.; Geiser, U.; Wang, H. H.; Carlson, K. D.; Williams, J. M.; Kwok, W. K.; Vandervoort, K. G.; Thompson, J. E.; Stupka, D. L.; Jung, D.; Whangbo, M. H. *Inorg. Chem.* **1990**, 2555. (c) Williams, J. M.; Kini, A. M.; Wang, H. H.; Carlson, K. D.; Geiser, U.; Montgomery, L. K.; Pyrka, G. J.; Watkins, D. M.; Kommers, J. M.; Boryschuk, S. J.; Crouch, A. V. S.; Kwok, W. K.; Schirber, J. E.; Overmyer, D. L.; Jung, D.; Whangbo, M. H. *Inorg. Chem.* **1990**, 3272.

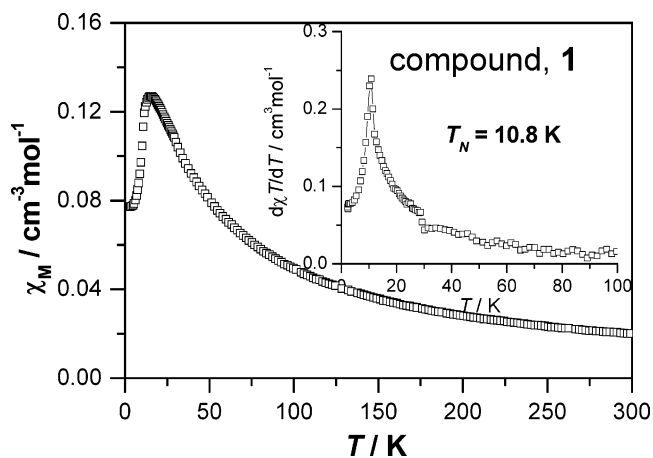


Figure 8. Temperature dependence of χ_M for **1** (inset: $d(\chi_M T)/dT$ vs T for **1**).

2D triangle layers constructed by 1,5- μ_2 -dca and μ_3 -dca, and the coligands of pzdo and 2-mpdo act as terminal ligands. However, in **1**, 2,5-dmpdo serves as a bridging ligand in the *trans* mode. The addition of one methyl group to the pyrazine ring changes the coordination mode of the coligands and results in a 3D α -Po-type network containing rarely observed 1,3- μ_2 -dca bridges. When more methyl groups are added to the pyrazine ring, the enhanced steric hindrance of 2,3,5-tmpdo and 2,3,5,6-tmpdo reduces their coordination ability. Therefore, they act as hydrogen bond acceptors in the lattice but not coordinating ligands. In these two cases, the small coordinating ligand, water, existing in the synthesis systems coordinates to the Co-dca frameworks. The resultant networks constructed by 1,5- μ_2 -dca are novel 2D double layers in **2** or common (4, 4) layers in **3**. These results indicate that the pyrazine-dioxide derivatives can diversify the polymeric topology of the framework as well as the coordination mode of dca.

Magnetic Properties of 1–3. The temperature dependence of the magnetic susceptibility, χ_M , (per two Co) for **1** in a field of 10 kOe is shown in Figure 8. With a decrease in temperature, χ_M increases gradually, reaching a maximum value of $0.127 \text{ cm}^3 \text{ mol}^{-1}$ at 15.3 K and then decreases, indicating antiferromagnetic coupling between the $\text{Co}(\text{II})$ ions. The magnetic data above 15 K can be fitted to the Curie–Weiss law with $C = 6.61 \text{ cm}^3 \text{ mol}^{-1} \text{ K}$ and $\theta = -33.5 \text{ K}$. At room temperature, $\chi_M T$ has a value of $6.03 \text{ cm}^3 \text{ mol}^{-1} \text{ K}$, which is obviously larger than the expected spin-only value of $3.75 \text{ cm}^3 \text{ mol}^{-1} \text{ K}$ for two noninteracting spin-only $\text{Co}(\text{II})$ ions with $S = 3/2$, indicating the unquenched orbital contribution. The Neel temperature, T_N , was determined from the sharp peak of $d(\chi_M T)/dT$ at 10.8 K (inset of Figure 8).²² Although compound **1** has a 3D structure, the antiferromagnetic ordering does show a low-dimensional characteristic because the ratio of $T_N/T(\chi_{\text{max}}) = 0.706$ is much lower than a 3D one.²³

The field dependence of the magnetization of **1** measured at 1.8 and 5 K, below T_N (10.8 K), shows a nearly linear

(22) (a) Fisher, M. E. *Proc. R. Soc. London, Ser. A* **1960**, 254, 66. (b) Fisher, M. E. *Philos. Mag.* **1962**, 7, 1731.

(23) DeFotis, G. C.; Remy, E. D.; Scherrer, C. W. *Phys. Rev. B* **1990**, 41, 9047.

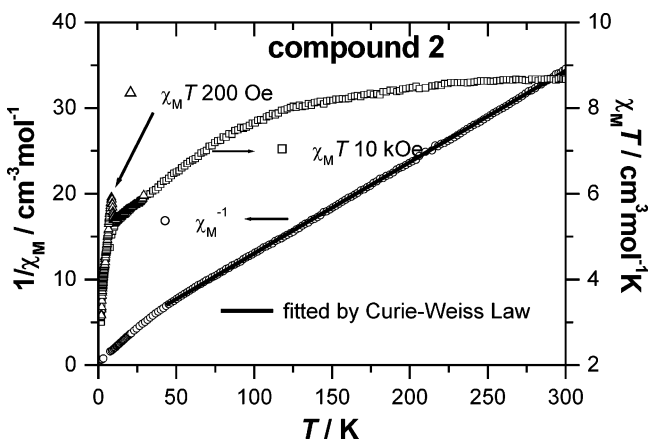


Figure 9. Temperature dependence of $\chi_M T$ and $1/\chi_M$ for **2**.

slow increase, suggesting antiferromagnetic ordering (Figure S5). The magnetization at 70 kOe at 1.8 K is only $1.11 N\beta$ (per two Co), far from the saturation value of ca. $6 N\beta$ that is expected for two $S = 3/2$ spins, this being the evidence that supports antiferromagnetic ordering. The $M-H$ plot measured at 15 K, which is above the ordering temperature, shows a linear increase, which increases much faster than that measured at 1.8 and 5 K, indicating that the increase of temperature breaks antiferromagnetic ordering.

The magnetic behavior of **1** is quite different from the reported compounds containing dca and pzdo or 2-mpdo, which display long-range ferromagnetic ordering below 2.5 K.^{10b} The ferromagnetic ordering found in these compounds results from the existence of tridentate dca coordination. The antiferromagnetic ordering in **1** is due to the spatial dimensionality and/or the bridging ligand of 2,5-dmpdo, which may transport antiferromagnetic coupling.¹²

The magnetic susceptibility of **2** versus temperature under a field of 10 kOe was shown in Figure 9, where χ_M is the susceptibility per $[Co_3]$ unit. The magnetic data above 50 K can be fitted by the Curie–Weiss Law with $C = 9.37 \text{ cm}^3 \text{ mol}^{-1} \text{ K}$ and $\theta = -22.2 \text{ K}$. The $\chi_M T$ value at room temperature is $8.80 \text{ cm}^3 \text{ mol}^{-1} \text{ K}$, which is comparable to the average experimental value of $9 \text{ cm}^3 \text{ mol}^{-1} \text{ K}$ for three octahedral Co(II) ions. With a decrease in temperature, $\chi_M T$ decreases gradually down to ca. 12 K and then decreases rapidly. The slow decrease above 12 K is a typical manner of an orbitally degenerate ${}^4T_{1g}$ (d^7 octahedral) system undergoing spin–orbit coupling.²⁴ The rapid decrease below 12 K suggests the possibility of antiferromagnetic coupling. The rapid increase in $\chi_M T$ occurring at ca. 9 K with an applied low field of 200 Oe is reminiscent of the onset of magnetic order. In the ac susceptibility of **2** (Figure S6), the in-phase signal increases with decreasing temperature, displays a small shoulder at ca. 9 K, and then increases to 2 K. The out-of-phase signal also gives small nonzero value at ca. 9 K, which also suggests the onset of magnetic ordering. Because the compounds of dca containing coligands are easily contaminated with their 3D α -M(dca)₂, as in our recent paper and the paper of Batten and Murray,¹⁰ we may reasonably assume that the observation of the transition at

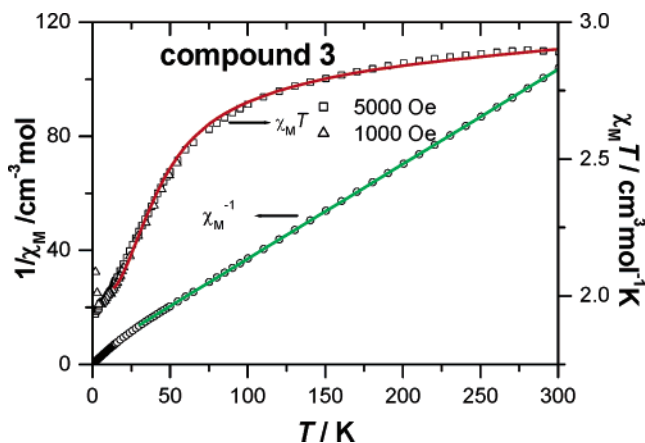


Figure 10. Temperature dependence of $\chi_M T$ and $1/\chi_M$ for **3**. The red line shows the fitting result by considering a mononuclear Co^{2+} with spin–orbit coupling in a molecular-field approximation. The green line shows the Curie–Weiss fitting.

ca. 9 K could be regarded as a result of trace 3D α -Co(dca)₂, which has critical temperature of 9 K, rather than any intrinsic ordering. The field dependence of the magnetization of **2** measured at 1.8 K shows a nearly linear increase below 25 kOe and reaches a value of $9.09 N\beta$ at 70 kOe (Figure S7).

The magnetic susceptibility of **3** versus temperature at a field of 5 kOe is shown in Figure 10, where χ_M is the susceptibility per Co(II) ion. The $\chi_M T$ value is $2.89 \text{ cm}^3 \text{ mol}^{-1} \text{ K}$ at 300 K, which is significantly larger than the spin-only value of $1.875 \text{ cm}^3 \text{ K mol}^{-1}$ and decreases upon cooling to $2.00 \text{ cm}^3 \text{ mol}^{-1} \text{ K}$ at 2 K. The magnetic susceptibility above 30.0 K obeys the Curie–Weiss law with the Weiss constant, $\theta = -11.5 \text{ K}$, and the Curie constant, $C = 3.01 \text{ cm}^3 \text{ mol}^{-1} \text{ K}$. The high value of C ($1.875 \text{ cm}^3 \text{ K mol}^{-1}$ for spin-only Co^{2+}) and the negative θ value may be due to the spin–orbit coupling, which is remarkable for the ${}^4T_{1g}$ state of Co^{2+} in an octahedral ligand field. From the fitted Curie constant, C , one can deduce the g value to be about 2.54. From the structure information, we know that the Co(II) ions are well separated, so we can treat the magnetic data by considering a mononuclear Co^{2+} with a spin–orbit coupling parameter λ ($H = -\lambda LS$) in a molecular-field approximation. The χ_{mono} for mononuclear Co^{2+} in an octahedral environment can be calculated from eq 1,²⁵

$$\chi_{\text{mono}} = \frac{1}{T} \left[\frac{7(3-A)^2 x}{5} + \frac{12(2+A)^2}{25A} + \left(\frac{2(11-2A)^2 x}{45} + \frac{176(2+A)^2}{675A} \right) x \exp\left(\frac{-5Ax}{2}\right) + \left(\frac{(5+A)^2 x}{9} - \frac{20(2+A)^2}{27A} \right) \exp(-4Ax) \right] / \left\{ \frac{8x}{3} \left[3 + 2 \exp\left(\frac{-5Ax}{2}\right) + \exp(-4Ax) \right] \right\} \quad (1)$$

with $x = \lambda/k_B T$. The parameter A gives a measure of the crystal field strength relative to the interelectronic repulsions

(24) Kahn, O. *Molecular Magnetism*; VCH: New York, 1993.

(25) Figgis, B. N.; Gerloch, M.; Lewis, J.; Mabbs, F. E.; Webb, G. A. *J. Chem. Soc. A* **1968**, 2086–2093 and references therein.

and is equal to 1.5 for a weak crystal field, 1.32 for a free ion, and 1.0 for a strong field. Considering the molecular-field approach with zJ as the total exchange coupling between Co^{2+} ions, we can fit our experimental data with eq 2:²⁴

$$\chi = \frac{\chi_{\text{mono}}}{1 - (2zJ/Ng^2\beta^2)\chi_{\text{mono}}} \quad (2)$$

In eqs 1 and 2, N , g , β , k_B and T have their usual meanings. The best fitting of the susceptibility data in the temperature range of 15 to 300 K gives $\lambda = -92 \text{ cm}^{-1}$, $A = 1.08$, and $zJ = 1.07 \text{ cm}^{-1}$ with $R = 3.2 \times 10^{-5}$ [$R = [\sum(\chi_{\text{obs}} - \chi_{\text{calcd}})^2 / \sum(\chi_{\text{obs}})^2]$]. The positive zJ value indicates the overall ferromagnetic coupling between the $\text{Co}(\text{II})$ ions. The $\chi_{\text{M}}T$ versus T plot under a low magnetic field of 1 kOe shows a slight increase below 5 K, which also suggests the possible weak ferromagnetic coupling between the $\text{Co}(\text{II})$ ions.

Conclusions

Three cobalt complexes based on dca with 2,5-dmpdo for **1**, 2,3,5-tmpdo for **2**, and 2,3,5,6-tmpdo for **3** have been synthesized and structurally and magnetically characterized. **1** contains 1,3- μ_2 - and 1,5- μ_2 -dca, presenting the first example with both of these kinds of dca bridges. **1** has an α -Po-type network consisting of Co-dca (4, 4) layers pillared by 2,5-dmpdo. **2** has a unique 2D double layer that is constructed by 1,5- μ_2 -dca and described as a twinned (4, 4) net. The 2D sheets are linked further by Co–H₂O–Co linkages to a 3D

framework with noncoordinated 2,3,5-tmpdo occupying the interstices. **3** has the usual (4, 4) Co-dca sheets with 1,5- μ_2 -dca bridges, and these sheets are separated by organic 2,3,5,6-tmpdo layers. The results of this work and previously reported ones revealed that pzdo with fewer methyl substituent pzdo's (2-mpdo, 2,5-dmpdo) can act as coligands, whereas more methyl substituent ones (2,3,5-tmpdo and 2,3,5,6-tmpdo) are noncoordinated probably because of the large spacial hindrance for coordination under similar synthesis conditions. However, the later ones still show their effect on the final solid structures via H bonds or other factors such as π – π stacking. **1** exhibits long-range antiferromagnetic ordering below 10.8 K because of the 3D structure constructed by 1,3- μ_2 -dca, 1,5- μ_2 -dca, and μ -2,5-dmpdo. However, compounds **2** and **3** are paramagnetic with antiferromagnetic coupling for **2** and ferromagnetic coupling for **3** between the metal centers.

Acknowledgment. This work was supported by the National Natural Science Foundation of China (nos. 20125104, 20221101, 20490210, and 90201014), the National Key Project for Fundamental Research (2003CCA00800).

Supporting Information Available: An X-ray crystallographic file in CIF format of compounds **1–3** and a PDF file containing more structural and magnetic figures (Figures S1–S7). This material is available free of charge via the Internet at <http://pubs.acs.org>.

IC048342J